

PAPER • OPEN ACCESS

Synthesis and characterization of nano rosette TiO_2 and $\text{CH}_3\text{NH}_3\text{PbCl}_2\text{I}$ for potential use in perovskite solar cell

To cite this article: N Sofyan *et al* 2019 *IOP Conf. Ser.: Mater. Sci. Eng.* **541** 012048

View the [article online](#) for updates and enhancements.

Synthesis and characterization of nano rosette TiO₂ and CH₃NH₃PbCl₂I for potential use in perovskite solar cell

N Sofyan¹, A Ridhova¹, Salman¹, A H Yuwono¹, A Udhiarto²

¹Department of Metallurgical and Materials Engineering, Faculty of Engineering, Universitas Indonesia, Depok 16424 Indonesia

²Department of Electrical Engineering, Faculty of Engineering, Universitas Indonesia, Depok 16424, Indonesia

E-mail : nofrijon.sofyan@ui.ac.id

Abstract. The characteristics of nano rosette TiO₂ hydrothermally grown on a glass substrate with potential application in perovskite solar cell has been examined. Nano rosette TiO₂ was synthesized through deposition on top of a fluorine-doped tin oxide glass substrate via hydrothermal reaction at 170°C for 6 hours. Formation and growth mechanism were characterized using X-ray diffraction (XRD), whereas the morphology was examined using a field emission scanning electron microscope (FE-SEM). The results showed that the formation of nano rosette TiO₂ has been completed after 6 hours. Structural study from X-ray diffraction also showed that the crystal structure formation has been completed after 6 hours. This nano rosette TiO₂ was tested for its performance as an electron transport layer (ETL) in the perovskite solar cell device. For this purpose, the perovskite CH₃NH₃PbCl₂I 0.8 M was deposited on top of the ETL layer and the performance was tested using a semiconductor parameter analyser (SPA). The result showed an efficiency of about 3.4%, which is promising for the next development.

1. Introduction

High energy requirements continue to drive intensive research in the field of solar cells. One of the latest generations of solar cells is perovskite solar cell (PSC), some of which still focus on the utilization of perovskite structured compounds, especially of lead-inorganic organic hybrids [1]. Perovskite compound was discovered in 1839 by Gustav Rose on the chemical compound CaTiO₃ with the general formula of ABX₃, where A and B are cations of normally different radius sizes, whereas X is an anion binding to both cations [2]. The compound with this perovskite structure could be used as an active layer of light catcher in a solar cell device, which is then converted into electrons to generate electrical current.

The efficiency of the PSC has grown tremendously since it was first recorded in 2009 of 3.8% until 2017 at around 22.7% and it is still expected to continue to increase as new progress in the area emerges [3]. Many investigators have put their efforts in the improvement of the PSC. For examples, Xiao et al. [4] have reported that the use of a combination of TiO₂ compact layers with the growth of TiO₂ nanorods as electron transporting layer (ETL) and partial substitution of CH₃NH₃I (MA-I) with MA-Br was able to increase the efficiency of PSC. Govindasamy et al. [5] reported that the addition of acetic acid to TiO₂ during chemical bath deposition process decreased the activation energy of the material. Liu and Aydil [6] have also reported that the addition of NaCl and two-step hydrothermal route could restraint the



growth of nanorods during the synthesis and improved the electron transfer efficiency of the PSC device. In another work, Jin et al. [7] have also found that by partial substitution of PbI_2 with 3% ZnCl_2 in the perovskite layer was capable of increasing the electron transport properties and increasing the efficiency of the PSC device.

Based on the aforementioned description, it can be understood that the structure and orientation of the semiconductor material in the PSC can improve the electron transfer process and thus the efficiency of the PSC device. Meanwhile, efficiency can be increased even more by substituting partial substitution of perovskite coating compounds. Therefore, a method that can combine the existing methods to improve PSC efficiency is needed. In this work, we combined the two methods, namely the use of combination of compact layers of TiO_2 nano rosette as an ETL and partial substitution of perovskite coating compounds by mixing the precursors of lead (II) chloride (PbCl_2) and methylammonium iodide ($\text{CH}_3\text{NH}_3\text{I}$) to form $\text{CH}_3\text{NH}_3\text{PbCl}_2\text{I}$.

2. Experimental Setup

2.1. Materials

The precursors were titanium tetra isopropoxide (TTIP, $\geq 97.0\%$, Sigma-Aldrich) and hydrochloric acid (HCl 37%, Merck) all with analytical grade reagents and used without further purification. For the solvents, acetone, ethanol and distilled water were used throughout the experiment except stated otherwise.

2.2. Preparation of Nano Rosette TiO_2

The synthesis of nano rosette TiO_2 was performed through deposition on top of a fluorine-doped tin oxide (FTO, $30 \Omega/\text{cm}^2$) glass substrate via modified hydrothermal reaction similar to the previously reported procedure by others [4]. The process was begun by mixing distilled water with hydrochloric acid in a beaker glass at a fix volume ratio of 1:1 to reach a total volume of 40 mL at room temperature condition. The solution was mixed under a magnetic stirrer for 5 minutes before being added with a volume of 450 μL TTIP and the agitation was continued for another 5 minutes to get a clear solution.

Meanwhile, the glass substrate was prepared by firstly cleaning it ultrasonically in a mixed solution of distilled water, acetone, and ethanol with volume ratios of 1:1:1 for 10 minutes. The cleaned substrate was placed horizontally at the bottom of 100 mL Teflon-lined stainless-steel autoclave before being poured with the previous TTIP prepared solution. The synthesis was conducted at 170°C for 6 hours in a vacuum oven (DZF-6050, Berkeley Scientific). After the synthesis, the autoclave was cooled to room temperature under flowing water for approximately 5 minutes. The glass substrate was then taken out and rinsed with distilled water and allowed to dry in air for 15 minutes before being calcined using hot-plate (Cimarec SP 131320-33, Thermo Scientific) at 450°C for 90 minutes and ready for the characterization.

2.3. Device Fabrication

The perovskite layer acting as an absorber was deposited on top of nano rosette TiO_2 layer through a solution drop and spin-coating process (K-359SD-1 Spinner, Kyowa Riken). Perovskite $\text{CH}_3\text{NH}_3\text{PbCl}_{3-x}\text{I}_x$ 0.8 M where $x = 1$ was obtained by mixing precursors of lead (II) chloride (PbCl_2 , Merck) and methylammonium iodide ($\text{CH}_3\text{NH}_3\text{I}$, Greatcell Solar) with a mass ratio of 1 : 3, i.e. 278 mg of PbCl_2 and 470 mg $\text{CH}_3\text{NH}_3\text{I}$ in 5 mL dimethylformamide (DMF, Merck) at 80°C under a magnetic stirrer for 2 hours. A 50 μL of this perovskite solution was dropped onto synthesized nano rosette TiO_2 layer and allowed to stand for 1 minute before being spin-coated at 3000 rpm for 30 seconds to remove the residual solvent. The perovskite layer from the spin-coating deposition was the calcined in a muffle furnace (LEF-1xxS type, Labtech) at 150°C for 60 minutes.

The hole transport layer was further deposited on top of the perovskite layer. This layer consisted of 80 mg of Spiro-OMeTAD (Greatcell Solar) dissolved in 1 mL of chlorobenzene. This solution was dropped on top of the perovskite layer and spin-coating was performed at 3000 rpm for 30 seconds.

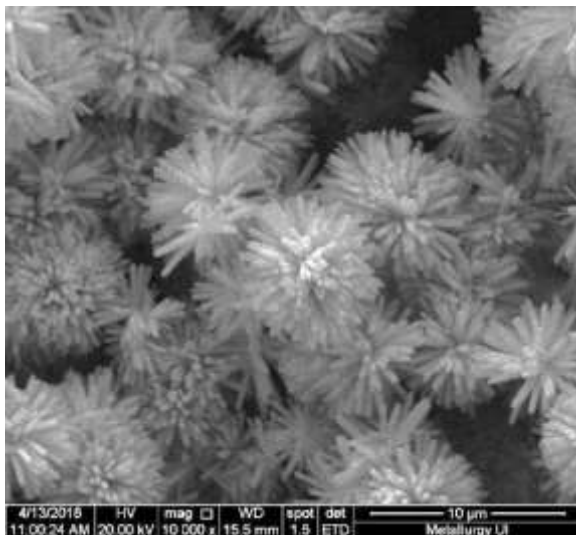
The last layer, the gold metal electrode, was deposited using sputter coater (SC7620 Sputter Coater, Quorum) under a pressure of 10^{-1} mbar and a current of 10 mA for 120 seconds following the pattern on the FTO glass. The device was then ready for performance characterization.

2.4. Characterization

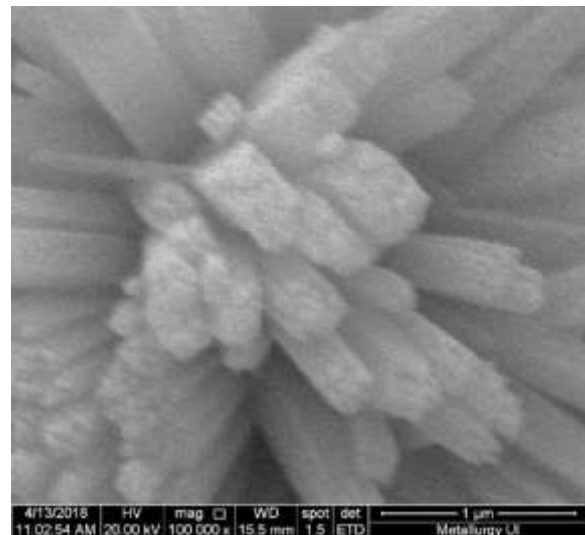
The morphology of the reaction product was examined using a field emission scanning electron microscope (FE-SEM, FEI Inspect F50) whereas the structural characteristics of the sample was observed using an X-ray diffractometer (XRD, PANalytical X'Pert PRO) operating at 40 kV 30 mA with Cu K α radiation ($\lambda = 1.5406 \text{ \AA}$). Device performance was measured through an I-V curve characteristic using a semiconductor parameter analyser. All characterizations were performed under an ambient condition with no control on environmental humidity and or pressure.

3. Results and Discussion

The morphology of TiO₂ hydrothermally synthesized at 170°C for 6 hours was studied through secondary electron images. Figure. 1 shows the morphology of the product in the forms of nano rosette TiO₂ under different conditions. As can be seen in Figure. 1, complete formation of nano rosette has been obtained at 6 hours of hydrothermal reaction time. Figure. 1(a) and 1(b) are the as-synthesized nano rosette TiO₂ at two different magnifications, whereas Figure. 1(c) and 1(d) are morphology of the nano rosette TiO₂ after being calcined at 450°C for 90 minutes. Not much differences that can be observed from these two morphologies except that at higher magnification, the one that has been calcined has sharp and smooth surface morphology. This could be because of the calcination process has resulted in the crystalline form of the nano rosette. After the completion of reaction time, the petal of the rosette has reached an average size of about 200 nm. These results are in agreement with our previous results [8].



(a)



(b)

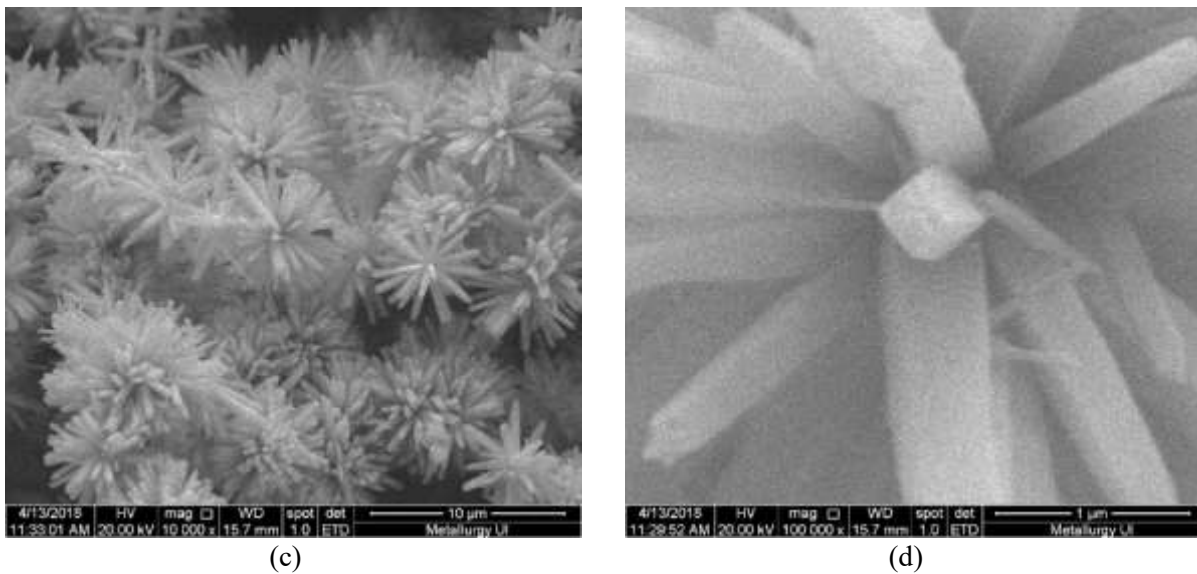


Figure 1. Secondary electron image of nano rosette TiO_2 hydrothermally synthesized at $170\text{ }^\circ\text{C}$ for 6 hours: (a) as-synthesized at low magnification, (b) as-synthesized at high magnification, (c) calcined at $450\text{ }^\circ\text{C}$ for 90 minutes at low magnification, and (d) calcined at $450\text{ }^\circ\text{C}$ for 90 minutes at high magnification. Low magnification has the bar scale of $10\text{ }\mu\text{m}$ and high magnification has the bar scale of $10\text{ }\mu\text{m}$.

In order to examine that the nano rosette has formed a more crystalline phase after the calcination process, X-ray diffraction examination has also been performed and the results are given in Figure. 2. As can be seen in Figure. 2(a), the pattern is X-ray diffractogram of rutile TiO_2 reference (JPDS 01-082-0154), Figure. 2(b) is diffractogram of the as-synthesized of hydrothermally grown TiO_2 , and Figure. 2(c) is the calcined diffractogram of hydrothermally grown TiO_2 .

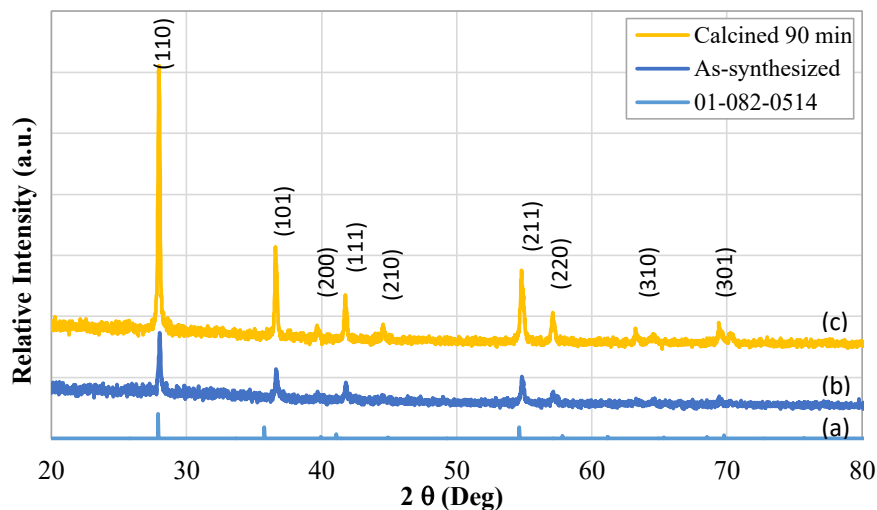


Figure 2. X-ray diffractograms of (a) rutile TiO_2 reference (JPDS 01-082-0154), (b) as-synthesized, and (c) calcined at $450\text{ }^\circ\text{C}$ for 90 minutes of the hydrothermally grown nano rosette TiO_2 for 6 hours.

The diffractogram of the as-synthesized nano rosette TiO_2 , as can be seen in Figure. 2(b), the phase form has shown a complete structure of crystalline phase but it is still with low intensity. All peaks have been identified and show the trend and confirmed the pure rutile crystal structure (JCPDS file No. 01-082-0514) indexed to tetragonal $P4_2/mnm$. Some peaks, however, shift to high angle due to the differences in the lattice parameters. There are four distinct diffraction peaks observed at 2θ 27.659°, 36.579°, 41.742°, and 54.776° corresponding to (110), (101), (111), and (211) of rutile crystal planes, respectively. No other characteristic peaks of other phases and or impurities are detected in the diffractograms. This tendency would be understandable since the formation of nano rosette TiO_2 has been completed. After calcination, the intensity has increased and has shown most of the corresponding peaks. Calculation using Scherrer formula [9] results in an average crystallite size of about 77 nm.

For the peak shifting, refinement of the crystal structure has been carried out using an initial input from the known lattice parameters of the rutile reference with $a = 4.508 \text{ \AA}$ and $c = 3.027 \text{ \AA}$. The results of calculation showed that the lattice parameters of the obtained nano rosette TiO_2 are $a = 4.557(6) \text{ \AA}$ and $c = 2.940(5) \text{ \AA}$. This finding agrees with the results found by others [10].

Morphology of the perovskite layer deposited on top of the nano rosette TiO_2 was observed before being coated using gold metal electrode. Figure. 3a shows low magnification backscattered electron images (bar scale 100 μm) of the perovskite layer coated on top of the nano rosette TiO_2 hydrothermally synthesized at 170°C for 6 hours. Inset in Figure. 3a is high magnification backscattered electron image with bar scale 2 μm . The morphology reveals the profile of the perovskite layer on top of the nano rosette TiO_2 . As can be seen from the Figure, the formation of perovskite layer has not been completely homogeneous indicated by uncovered area of nano rosette TiO_2 . Moreover, as can be seen in Figure. 3(b), the spectrum of energy dispersive X-ray spectroscopy from the backscattered image is still showing the presence of titanium element indicated that some areas on the surface of the electron transport layer have not been fully covered by the perovskite layer. Hence, this deposition process still needs to be further optimized. Nonetheless, the performance of this result has been tested and the result is given in Figure. 4.

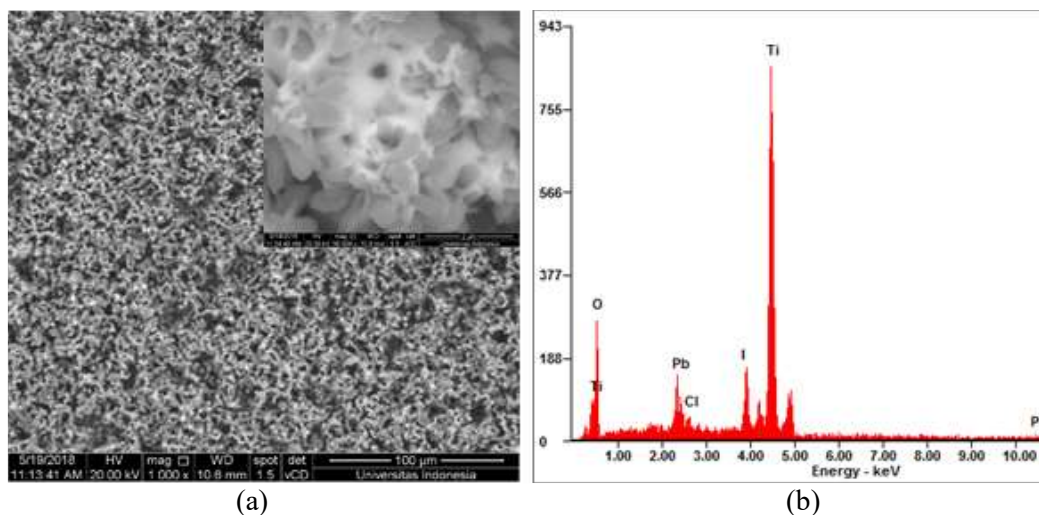


Figure 3. (a) Backscattered electron image of the perovskite layer coated on top of nano rosette TiO_2 hydrothermally synthesized at 170°C for 6 hours at low magnification (bar scale 100 μm). Inset is the high magnification backscattered electron image (bar scale 2 μm) revealing the profile of the perovskite layer on top of the nano rosette. (b) Energy dispersive X-ray spectroscopy spectrum shows the detected elements of the backscattered image.

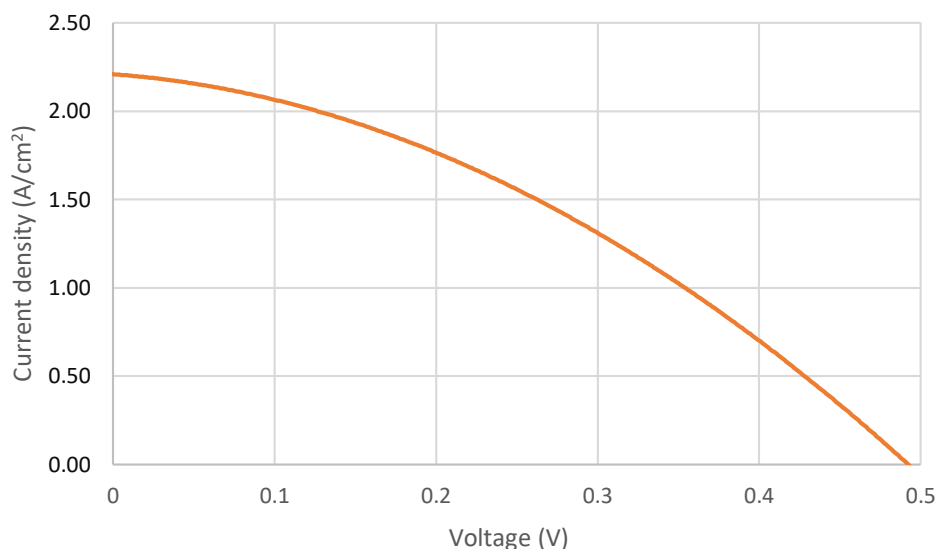


Figure 4. I-V curve characteristics of the PSC device fabricated from nano rosette TiO₂ hydrothermally synthesized at 170 °C for 6 hours.

Power conversion efficiency was calculated based on this I-V curve characteristic, in which [11]:

$$\eta = \frac{FF \times I_{sc} \times V_{oc}}{I_{in}} \times 100 \quad (1)$$

where I_{sc} is the short-circuit photocurrent density (A cm⁻²), V_{oc} is the open-circuit voltage (volts), I_{in} is the intensity of the incident light (W cm⁻²) and FF is the fill factor defined as

$$FF = \frac{I_{max} V_{max}}{I_{sc} V_{oc}} \quad (2)$$

where I_{max} and V_{max} are maximum photocurrent and voltage, respectively. Their values can be extracted from the maximum power of the I-V characteristics. Based on the data obtained from the photocurrent-voltage examination of the PSC device, the maximum power conversion efficiency (PCE) is found to be 3.4%. Compared to the existing efficiency [3], this value is still relatively low. This low value is expected because of inhomogeneous distribution of the perovskite layer that is yet to be improved, however, this current result is convincing and promising for the next development.

4. Conclusion

The characteristics of nano rosette TiO₂ grown on glass substrate via hydrothermal at different reaction time for potential use as electron transport layer in perovskite solar cell have been examined. Secondary electron images showed that the formation of crystal structure has been completed after 6 hours. X-ray diffractograms supported the morphological study in which after 6 hours of hydrothermal reaction time, the formation of nano rosette has been completed indicated by high intensity of the crystal structure indexed to rutile P4₂/mmm with lattice parameters of $a = 4.557(6)$ Å and $c = 2.940(5)$ Å. The performance of the materials used as electron transport layer in PSC tested using a semiconductor parameter analyser showed an efficiency of about 3.4%.

References

- [1] Niu G, Guo X and Wang L 2015 *J. Mater. Chem. A* **3** 8970

- [2] Giorgi G and Yamashita K 2015 *J. Mater. Chem. A* **3** 8981
Shaikh J S, Shaikh N S, Sheikh A D, Mali S S, Kale A J, Kanjanaboos P, Hong C K, Kime J H, Patil P S, *Mater. Design* 2017 **136** 54
- [3] Xiao G, Shi C, Li L, Zhang Z, Ma C, and Lv K 2017 *Ceram. Int.* **43** 12534
- [4] Govindasamy G, Murugasen P, Sagadevan S 2016 *Mater. Res.* **19**(2) 413
- [5] Liu B and Aydil E S 2009 *J. Am. Chem. Soc.* **131** 3985
- [6] Jin J, Li H, Chen C, Zhang B, Xu L, Dong B, Song H, and Dai Q 2017 *ACS Appl. Mater. Interfaces* **9** 42875
- [7] Sofyan N, Ridhova A, Yuwono A H, Wu J 2018 *Int. J. Technol.* **9**(6) 1196
- [8] Patterson A L 1939 *Phys. Rev.* **56** 978
- [9] Facchin G, Carturan G, Campostrini R, Gialanella S, Lutterotti L, Armelao L, Marci G, Palmisano L and Sclafani A 2000 *J. Sol-Gel Sci. Technol.* **18** 29
- [10] Fernando J M R C and Senadeera G K R 2008 *Curr. Sci.* **95** 663

Acknowledgments

This work is funded by the Directorate of Research and Community Services (DRPM) Universitas Indonesia through the grant of Hibah PITTA No. 2504/UN2.R3.1/HKP.05.00/2018.